




Intracellular autoactivation of TMPRSS11A, an airway epithelial transmembrane serine protease

Received for publication, May 25, 2020, and in revised form, July 14, 2020. Published, Papers in Press, July 15, 2020, DOI 10.1074/jbc.RA120.014525

Ce Zhang¹, Yikai Zhang^{1,2}, Shengnan Zhang^{1,2}, Zhiting Wang¹, Shijin Sun^{1,2}, Meng Liu¹, Yue Chen¹, Ningzheng Dong^{1,2,*}, and Qingyu Wu^{1,3,*} 

From the ¹Cyrus Tang Hematology Center, Collaborative Innovation Center of Hematology, State Key Laboratory of Radiation Medicine and Prevention, Soochow University, Suzhou, China, the ²MOH Key Laboratory of Thrombosis and Hemostasis, Jiangsu Institute of Hematology, the First Affiliated Hospital of Soochow University, Suzhou, China, and the ³Cardiovascular & Metabolic Sciences, Lerner Research Institute, Cleveland Clinic, Cleveland, Ohio, USA

Edited by Craig E. Cameron

Type II transmembrane serine proteases (TTSPs) are a group of enzymes participating in diverse biological processes. Some members of the TTSP family are implicated in viral infection. TMPRSS11A is a TTSP expressed on the surface of airway epithelial cells, which has been shown to cleave and activate spike proteins of the severe acute respiratory syndrome (SARS) and the Middle East respiratory syndrome coronaviruses (CoVs). In this study, we examined the mechanism underlying the activation cleavage of TMPRSS11A that converts the one-chain zymogen to a two-chain enzyme. By expression in human embryonic kidney 293, esophageal EC9706, and lung epithelial A549 and 16HBE cells, Western blotting, and site-directed mutagenesis, we found that the activation cleavage of human TMPRSS11A was mediated by autocatalysis. Moreover, we found that TMPRSS11A activation cleavage occurred before the protein reached the cell surface, as indicated by studies with trypsin digestion to remove cell surface proteins, treatment with cell organelle-disturbing agents to block intracellular protein trafficking, and analysis of a soluble form of TMPRSS11A without the transmembrane domain. We also showed that TMPRSS11A was able to cleave the SARS-CoV-2 spike protein. These results reveal an intracellular autocleavage mechanism in TMPRSS11A zymogen activation, which differs from the extracellular zymogen activation reported in other TTSPs. These findings provide new insights into the diverse mechanisms in regulating TTSP activation.

Type II transmembrane serine proteases (TTSPs) are a group of enzymes with a similar domain structural arrangement, including a short N-terminal cytoplasmic tail, a single-span transmembrane domain, and an extended extracellular region with various modules and a C-terminal trypsin-like protease domain (1, 2). TTSPs act in diverse tissues to participate in physiological and pathological processes, including iron metabolism (3, 4), liver metabolism (5), blood pressure regulation (6, 7), food digestion (8), auditory function (9, 10), vascular remodeling (11), epithelial development (12, 13), intestinal barrier function (14, 15), and cancer development (16, 17).

In recent years, TTSPs have been implicated in coronavirus (CoV) infection. In particular, TTSPs expressed in the human respiratory tract, including human airway trypsin-like protease (HAT) (18), the TTSP mosaic serine protease large form (19), differentially expressed in squamous cell carcinoma 1 (DESC1) (19), transmembrane protease serine 2 (TMPRSS2) (18, 20–26), and TMPRSS11A (27, 28), were shown to cleave the severe acute respiratory syndrome (SARS) CoV, the Middle East respiratory syndrome (MERS) CoV or SARS-CoV-2 spike (S) proteins in cell-based studies. As the S proteins are major determinants for receptor binding and membrane fusion in host cells (29), it appears that human airway TTSPs have been exploited by the CoVs to enhance their infectivity.

TTSPs are synthesized in a precursor or zymogen form with little catalytic activity. Proteolytic cleavage at a conserved activation site converts the zymogen to an active enzyme. To date, how CoV-activating TTSPs are activated in cells is not well understood. In this study, we analyzed the activation cleavage of TMPRSS11A, which is expressed in airway epithelial cells (28, 30) and activates SARS and MERS CoV S proteins (27, 28). By immunostaining, flow cytometry, Western blotting, protease digestion, and site-directed mutagenesis, we show that TMPRSS11A is autoactivated inside the cell before reaching the cell surface. This mechanism of intracellular activation cleavage differs from the extracellular activation cleavage reported in other TTSPs. Moreover, we found that TMPRSS11A exhibited the activity in cleaving the SARS-CoV-2 S protein.

Results

Cleavage of the conserved activation site in TMPRSS11A

Human TMPRSS11A consists of 418 amino acids. Fig. 1A shows the domain structure of TMPRSS11A, including an N-terminal cytoplasmic tail, a transmembrane domain (TM), and an extracellular region containing a SEA (sea urchin sperm protein/enteropeptidase/agrin) domain and a C-terminal serine protease domain. The conserved activation cleavage site is at Arg¹⁸⁶–Ile¹⁸⁷ (Fig. 1A and Fig. S1). There is a disulfide bond (Cys¹⁷⁵–Cys²⁹²) linking the protease domain to the propeptide region after the cleavage at the Arg¹⁸⁶–Ile¹⁸⁷ (Fig. 1A).

To study TMPRSS11A, we expressed human TMPRSS11A with a C-terminal V5 tag in transfected human embryonic kidney 293 (HEK293) cells. In flow cytometry, we found

This article contains supporting information.

*For correspondence: Ningzheng Dong, ningzhengdong@suda.edu.cn; Qingyu Wu, wuqy@ccf.org.

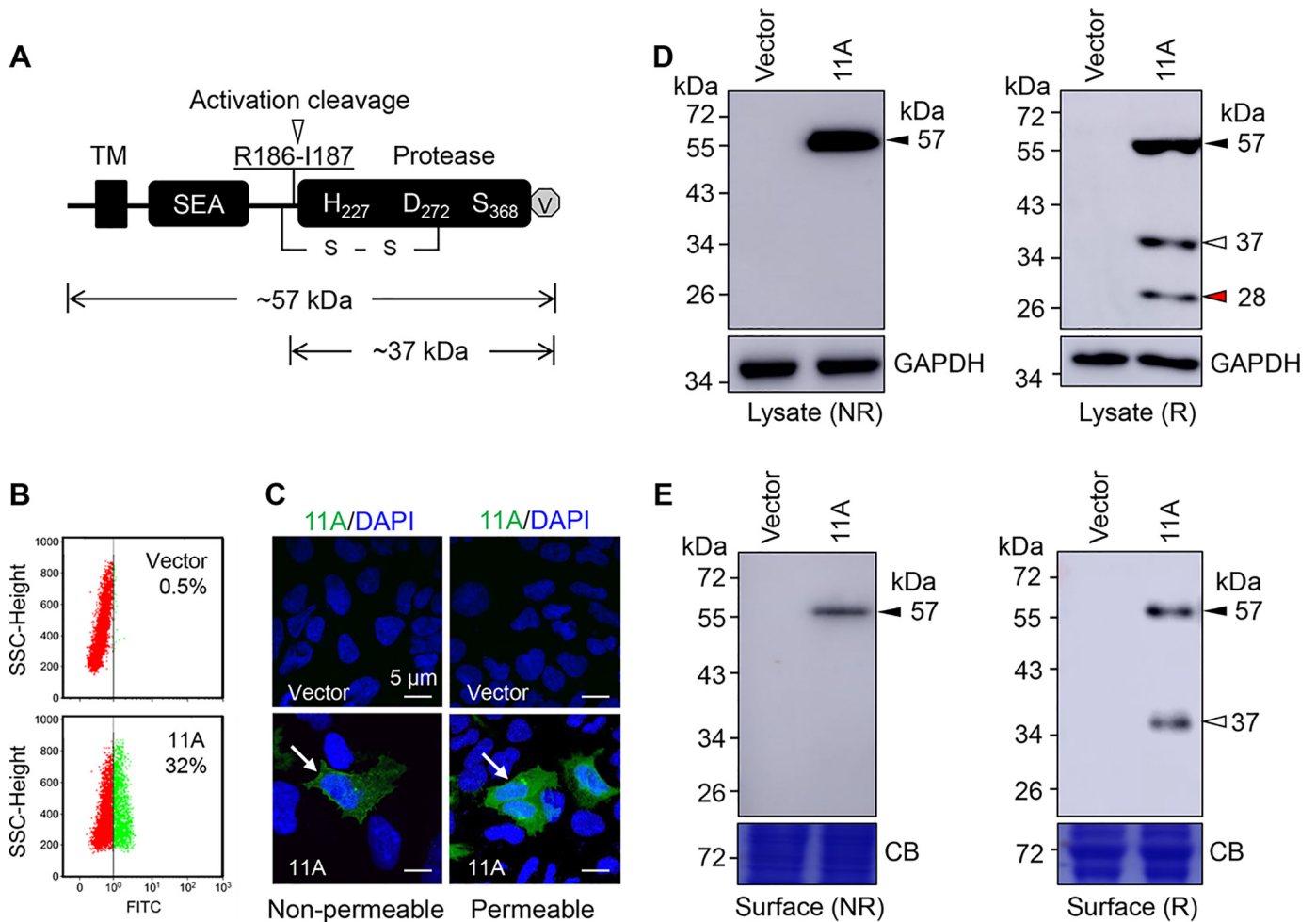


Figure 1. TMPRSS11A expression and cleavage in HEK293 cells. *A*, human TMPRSS11A protein consists of an N-terminal cytoplasmic tail, a TM domain, a SEA domain, and a C-terminal protease domain. The activation cleavage site is at Arg¹⁸⁶-Ile¹⁸⁷ (arrowhead). Catalytic residues in the protease domain and a disulfide bond (s-s) connecting the propeptide region and the protease domain are indicated. A V5 tag (v) is at the C terminus. Expected molecular masses for TMPRSS11A zymogen and the cleaved protease domain fragment are shown. *B*, flow cytometric analysis of TMPRSS11A on the surface of HEK293 cells transfected with a TMPRSS11A (11A)-expressing plasmid or a vector. Percentages of TMPRSS11A-positive cells are indicated. *C*, immunostaining of TMPRSS11A in nonpermeabilized and permeabilized HEK293 cells transfected with a TMPRSS11A (11A)-expressing plasmid or vector. Arrows indicate TMPRSS11A-positive cells. Scale bars, 5 μ m. *D* and *E*, Western blotting of TMPRSS11A proteins in lysates (*D*) and biotin-labeled surface proteins (*E*) from HEK293 cells transfected with a TMPRSS11A (11A)-expressing plasmid or a vector. Experiments were done under nonreducing (NR) or reducing (R) conditions with an anti-V5 antibody. TMPRSS11A fragments are indicated by arrowheads. GAPDH and Coomassie Blue (CB)-stained nonspecific bands were used as protein loading controls in the respective experiments. Data are representative of at least three experiments.

TMPRSS11A on the cell surface (Fig. 1*B*). In immunostaining, we detected TMPRSS11A on the surface of nonpermeabilized cells (Fig. 1*C*). The immunofluorescent signal was stronger when the cells were permeabilized, which allows staining both the cell surface and intracellular TMPRSS11A protein (Fig. 1*C*). These results are consistent with the predicted membrane topology of TMPRSS11A being a TTSP.

In Western blotting of lysates from the transfected HEK293 cells, we detected a single ~57-kDa band under nonreducing conditions (Fig. 1*D*, left panel). When Western blotting was done under reducing conditions, three bands of ~57, ~37, and ~28 kDa, respectively, were detected (Fig. 1*D*, right panel). In Western blotting with cell surface-labeled proteins, a single band (~57 kDa) and two bands (~57 and ~37 kDa) were detected under nonreducing and reducing conditions, respectively (Fig. 1*E*). Based on the calculated molecular mass, the ~57-kDa band represents the one-chain TMPRSS11A zymogen, whereas the ~37-kDa band represents the protease do-

main fragment cleaved at the conserved activation site (Fig. 1*A*). Because the V5 tag was at the C terminus, the cleaved N-terminal fragment was not detected by the anti-V5 antibody in Western blotting. These results indicate that TMPRSS11A is activated and present on the surface of the transfected HEK293 cells.

Identification of another cleavage site in the protease domain

The identity of the ~28-kDa band detected in Western blotting (Fig. 1*D*, right panel) was unclear. This band was observed under reducing conditions in cell lysates, but not among cell surface-labeled proteins (Fig. 1*E*, right panel), indicating that this fragment remained inside the cells. Human TMPRSS11A contains two *N*-glycosylation sites: one at Asn¹⁵³ in the SEA domain and the other at Asn³⁰³ in the protease domain (Fig. 2*A*). To exclude the possibility that the ~28-kDa band was an unglycosylated fragment, we treated HEK293 cell lysates with

TMPRSS11A zymogen activation

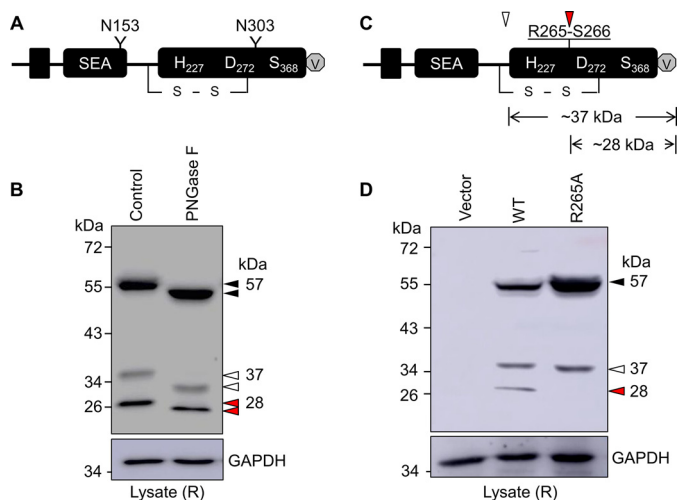


Figure 2. TMPRSS11A N-glycosylation and cleavage in the protease domain. A, illustration of N-glycosylation sites (Y shaped symbols) in human TMPRSS11A. B, Western blotting of TMPRSS11A fragments in cell lysates treated with control buffer or PNGase F. Western blotting was done under reducing (R) conditions with an anti-V5 antibody. Shifted bands after PNGase F treatment are indicated by double arrowheads. C, illustration of a potential cleavage site at Arg²⁶⁵-Ser²⁶⁶ (red arrowhead) in the TMPRSS11A protease domain. D, Western blotting of TMPRSS11A fragments in lysates from HEK293 cells transfected with a vector or plasmids expressing TMPRSS11A WT and the mutant R265A. Experiments were done under reducing (R) conditions with an anti-V5 antibody. TMPRSS11A fragments are indicated by arrowheads. GAPDH was used as a protein loading control. Data are representative of at least three experiments.

PNGase F to remove N-glycans on proteins. In Western blotting under reducing conditions, the ~57-, ~37-, and ~28-kDa TMPRSS11A bands all migrated faster compared with those in untreated samples (Fig. 2B), indicating that the ~28-kDa band may be a proteolytically cleaved fragment but not an unglycosylated fragment.

Based on the calculated molecular mass, the ~28-kDa band could be generated from a cleavage at Arg²⁶⁵ in the protease domain (Fig. 2C). To test this hypothesis, we made a plasmid expressing the mutant R265A, in which Arg²⁶⁵ in TMPRSS11A was replaced by Ala. In Western blotting with lysates from transfected HEK293 cells, the ~28-kDa band was detected in TMPRSS11A WT but not the mutant R265A (Fig. 2D), indicating that the ~28-kDa band is created by proteolytic cleavage at Arg²⁶⁵ in the protease domain.

Analysis of TMPRSS11A proteins with mutated activation cleavage and catalytic sites

In a recent study in transfected 293T cells, more than seven major TMPRSS11A fragments were detected by Western blotting (28). It is difficult to know if those fragments were derived by TMPRSS11A autocatalysis or unknown protease(s) or both in 293T cells. To circumvent this problem, we made plasmids expressing mutants R186A and S368A, in which the activation cleavage site at Arg¹⁸⁶ and the catalytic Ser³⁶⁸ were mutated to Ala, respectively (Fig. 3A). In Western blotting of lysates from HEK293 cells expressing the R186A mutant, only the ~57-kDa zymogen band was detected (Fig. 3B), indicating that the ~37-kDa band was derived from cleavage at the conserved activation site Arg¹⁸⁶ and that the single-chain

TMPRSS11A was incapable of cleaving at Arg²⁶⁵. Similarly, Western blotting of lysates from HEK293 cells expressing the S368A mutant showed the ~57-kDa band only (Fig. 3B), indicating that cleavages at Arg¹⁸⁶ (generating the ~37-kDa band) and Arg²⁶⁵ (generating the ~28-kDa band) depended on the catalytic activity of TMPRSS11A.

TMPRSS11A, also called ECRG1 (esophageal cancer-related gene 1), was first identified in human esophageal cancers (31, 32). To verify our results, we expressed TMPRSS11A WT and mutants R186A and S368A in EC9706 cells, a human esophageal cancer cell line (33). In Western blotting of lysates from transfected EC9706 cells, we detected three bands of ~57, ~37, and ~28 kDa, respectively, in TMPRSS11A WT, but a single ~57-kDa band in mutants R186A and S368A (Fig. 3C). Similar results were observed in additional experiments with human bronchial (16HBE) and alveolar basal (A549) epithelial cells (Fig. S2). These results are consistent, indicating that TMPRSS11A undergoes autoactivation at Arg¹⁸⁶ and subsequent autocleavage at Arg²⁶⁵ in the protease domain.

Intracellular cleavage of TMPRSS11A

To understand if the detected TMPRSS11A autoactivation cleavage occurred intracellularly or on the cell surface, we expressed TMPRSS11A WT in HEK293 cells and treated the cells with trypsin to remove surface proteins. In flow cytometry, TMPRSS11A was detected on the surface of the transfected HEK293 cells (Fig. 4A). The expression was reduced to the background level in the cells treated with trypsin (Fig. 4A). When the cells were lysed and lysates were analyzed by Western blotting, we observed the ~57-, ~37-, and ~28-kDa bands in the cells without or with trypsin treatment (Fig. 4B). These results indicate that TMPRSS11A activation cleavage occurred intracellularly.

We next treated HEK293 cells expressing TMPRSS11A with brefeldin A (BFA) and monensin, which inhibit protein trafficking in the endoplasmic reticulum (ER) and the Golgi (34). In Western blotting, we found the ~57-, ~37-, and ~28-kDa bands in TMPRSS11A-expressing cells without or with BFA or monensin treatment (Fig. 4C). In these studies, we did parallel control experiments with corin (Fig. S3), a TTSP known to be activated on the cell surface but not intracellularly (6). In Western blotting, the ~40-kDa corin protease domain fragment from activation cleavage was detected in the cells without, but not with, trypsin, BFA, or monensin treatment (Fig. 4D). These results indicate that, unlike corin, TMPRSS11A is activated intracellularly before reaching the cell surface.

Intracellular cleavage of soluble TMPRSS11A

To examine if the transmembrane domain in TMPRSS11A is required for activation cleavage, we made a plasmid expressing a soluble form of TMPRSS11A, in which the cytoplasmic tail and the transmembrane domain were replaced with the signal peptide of IgK (Fig. 5A) (35). In addition, we made another plasmid expressing an inactive soluble TMPRSS11A mutant (soluble S368A), in which the catalytic Ser³⁶⁸ was replaced by Ala (Fig. 5A). As expected, TMPRSS11A WT, but not soluble TMPRSS11A (s11A), was found on the surface of transfected

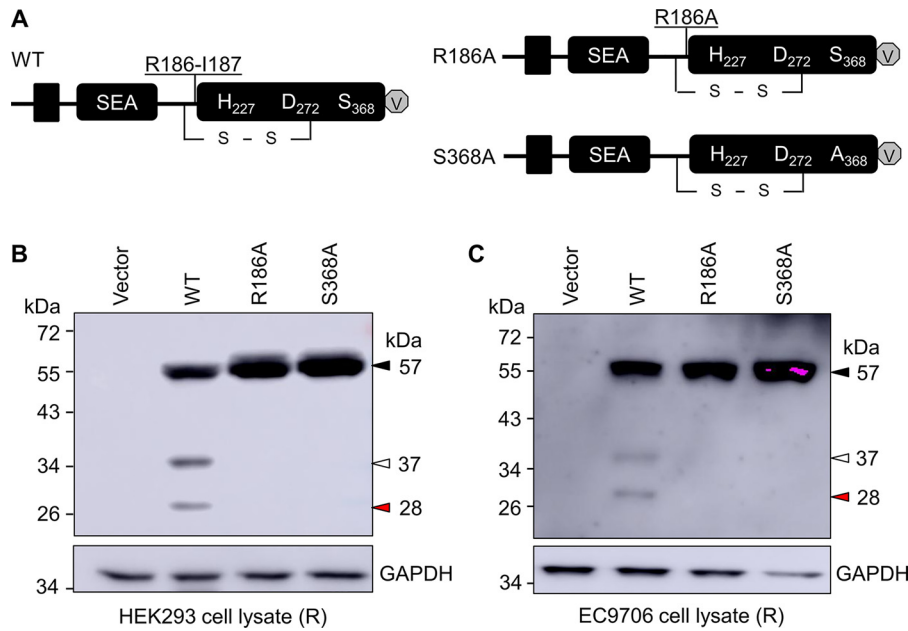


Figure 3. Analysis of inactive TMPRSS11A mutants R186A and S368A. A, illustration of TMPRSS11A WT and inactive mutants R186A (zymogen activation cleavage site) and S368A (active site). B and C, Western blotting of TMPRSS11A fragments in lysates from HEK293 (B) and EC9706 (C) cells transfected with a vector or plasmids expressing TMPRSS11A WT and mutants R186A and S368A. Western blotting was done under reducing (R) conditions with an anti-V5 antibody. TMPRSS11A fragments are indicated by arrowheads. GAPDH was used as a protein loading control. Data are representative of at least three experiments.

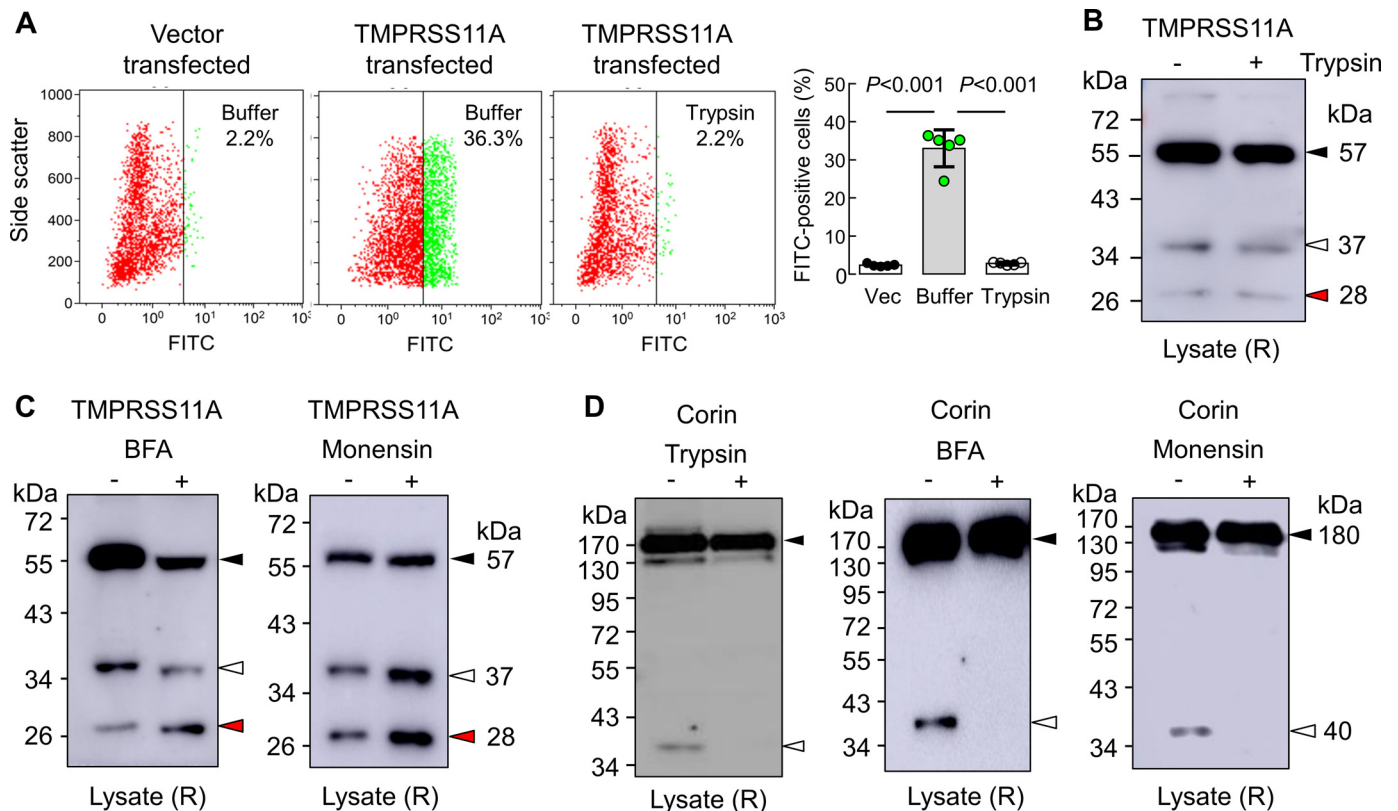


Figure 4. Analysis of TMPRSS11A and corin in HEK293 cells treated with trypsin, BFA, or monensin. A, HEK293 cells were transfected with a control vector and the plasmid expressing TMPRSS11A. TMPRSS11A-expressing cells were treated without or with trypsin. Cell surface TMPRSS11A expression was analyzed by flow cytometry with an anti-V5 antibody. Numbers indicate the percentages of TMPRSS11A-positive cells. Quantitative data of five experiments are shown in the bar graph with *p* values. B, HEK293 cells expressing TMPRSS11A were treated with buffer (control) (–) or trypsin (+) before being lysed for Western blotting under reducing (R) conditions. C, Western blotting of TMPRSS11A fragments in lysates from HEK293 cells treated with buffer (–) or BFA (left panel) or monensin (right panel) (+). Western blotting was done under reducing (R) conditions with an anti-V5 antibody. D, Western blotting of corin protein in HEK293 cells treated without (–) or with (+) trypsin (left panel), BFA (middle panel), or monensin (right panel). TMPRSS11A and corin fragments are indicated by arrowheads. Data are representative of at least three experiments.

TMPRSS11A zymogen activation

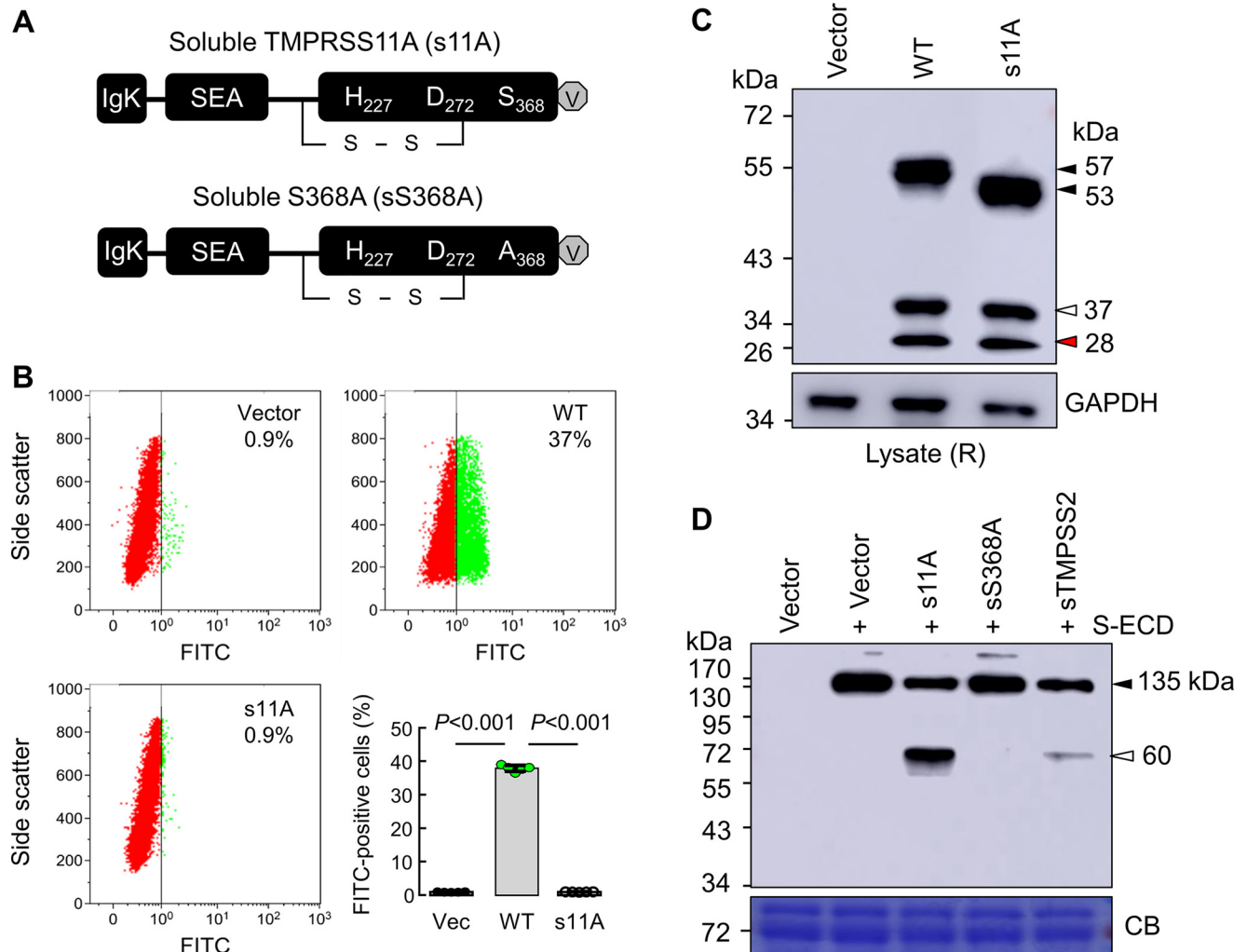


Figure 5. Expression and cleavage of a soluble form of TMPRSS11A. *A*, illustration of soluble forms of TMPRSS11A (s11A) and the mutant TMPRSS11A S368A (sS368A) with a signal peptide from IgK and the entire extracellular region. *B*, flow cytometry was done with an anti-V5 antibody to analyze TMPRSS11A on the surface of HEK293 cells transfected with a vector or plasmids expressing TMPRSS11A WT and s11A. Numbers indicate the percentages of TMPRSS11A-positive cells. Quantitative data from five experiments are shown in the bar graph with *p* values. *C*, Western blotting of TMPRSS11A fragments in lysates from HEK293 cells transfected with a vector or plasmids expressing TMPRSS11A WT and s11A. Western blotting was done under reducing (R) conditions with an anti-V5 antibody. TMPRSS11A fragments are indicated by arrowheads. *D*, recombinant SARS-CoV-2 S-ECD was incubated with the conditioned medium from HEK293 cells transfected with a vector or plasmids expressing s11A, sS368A, and a soluble form of TMPRSS2 (sTMPRSS2). Western blotting was done under reducing conditions with an anti-FLAG antibody. The uncleaved S-ECD fragment (filled arrowhead) and the cleaved ~60-kDa fragment (open arrowhead) are indicated. GAPDH and Coomassie Blue (CB)-stained nonspecific bands were used as protein loading controls in respective experiments. Data are representative of three experiments.

HEK293 cells in flow cytometry (Fig. 5B). In Western blotting, we found all three bands of ~57/53, ~37, and ~28 kDa, respectively, in lysates from HEK293 cells expressing TMPRSS11A WT and s11A (Fig. 5C), indicating that soluble TMPRSS11A undergoes similar intracellular activation cleavage and that the transmembrane domain is not required for TMPRSS11A autoactivation. We next incubated the conditioned medium containing s11A with a recombinant SARS-CoV-2 S protein fragment corresponding to the nearly entire extracellular region (residues 16-1213) produced from insect cells. We detected a ~60-kDa band (Fig. 5D), which is close to the calculated molecular mass of the cleaved S2 fragment (59 kDa). The ~60-kDa band was not detected in samples from vector-transfected cells or cells expressing the inactive soluble TMPRSS11A S368A (Fig. 5D). In a positive control, a similar ~60-kDa band was observed when we used the conditioned medium from cells

expressing a soluble form of TMPRSS2, which cleaves SARS-CoV-2 S protein (22) (Fig. 5D). We did not detect any SARS-CoV-2 S protein fragments of ~45 kDa, which is the calculated molecular mass of the S2' fragment. These results indicate that TMPRSS11A is capable of cleaving SARS-CoV-2 S protein at least *in vitro*.

Intermolecular cleavage of TMPRSS11A

The results described above support TMPRSS11A autoactivation. It was unclear if the autoactivation cleavage of TMPRSS11A occurs in *cis* (intramolecular) or in *trans* (intermolecular). To address this question, we further analyzed the soluble S368A mutant (sS368A) (Fig. 5A). In transfected HEK293 cells, sS368A was detected in the conditioned medium, as expected (Fig. 6A). On Western blots, the sS368A fragment in the conditioned medium had a higher

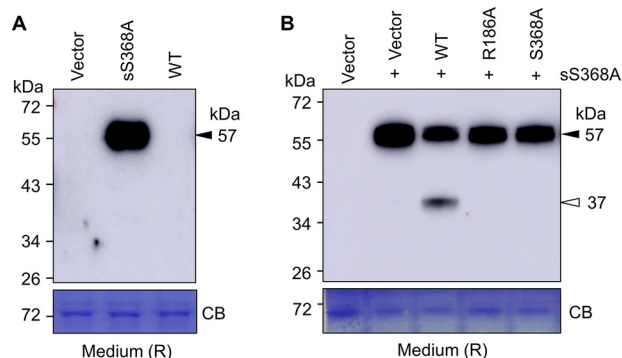


Figure 6. Expression and cleavage of the soluble TMPRSS11A mutant S368A. *A*, immunoprecipitation and Western blotting of TMPRSS11A protein in the conditioned medium from HEK293 cells transfected with a vector or plasmids expressing the sS368A mutant and TMPRSS11A WT. *B*, immunoprecipitation and Western blotting of TMPRSS11A protein in the conditioned medium from HEK293 cells transfected with a vector or the plasmid expressing the sS368A mutant together with a vector or plasmids expressing TMPRSS11A WT and mutants R186A and S368A. In Western blotting, an anti-V5 antibody was used. Coomassie Blue (CB)-stained nonspecific bands were used as a protein loading control. Data are representative of at least three experiments.

molecular mass than that in lysates (~ 57 versus ~ 53 kDa) (Fig. S4). When the samples were treated with PNGase F, the sS368A fragment from the conditioned medium and lysates migrated faster at ~ 53 and ~ 51 kDa, respectively (Fig. S4). The results suggest that other conformational changes or post-translational modifications may account for the higher molecular mass observed in the sS368A fragment from the conditioned medium.

We next transfected HEK293 cells with the plasmid expressing the sS368A mutant together with plasmids expressing TMPRSS11A WT and mutants R186A and S368A or a control vector. In Western blotting, the ~ 37 -kDa band derived from activation cleavage was observed in the conditioned medium from HEK293 cells co-expressing TMPRSS11A WT, but not mutants R186A and S368A (Fig. 6B), indicating that intermolecular cleavage of TMPRSS11A did occur under our experimental conditions. We then did another experiment, in which plasmid expressing the sS368A mutant was co-transfected with plasmids expressing TMPRSS11A, hepsin, TMPRSS2, and corin in HEK293 cells. In Western blotting of the conditioned medium, the ~ 37 -kDa band from the sS368A mutant was detected in samples from TMPRSS11A-, hepsin- and TMPRSS2-expressing, but not corin-expressing, cells. The levels of this band, however, were much lower in samples from hepsin- and TMPRSS2-expressing cells than that in TMPRSS11A-expressing cells (Fig. S5). These results support the idea of TMPRSS11A autoactivation, although the possibility that other TTSP-mediated transactivation cleavage may occur cannot be excluded.

Effects of HAI-1 and HAI-2 on TMPRSS11A activation cleavage

Hepatocyte growth factor activator inhibitors 1 and 2 (HAI-1 and HAI-2) are structurally related type I transmembrane serine protease inhibitors (36). Recently, HAI-1 was shown to inhibit HAT and DESC1, but not TMPRSS11A, activity in cell-based studies (28). To examine the effect of HAI-1 and HAI-2 on TMPRSS11A activation cleavage, we co-transfected

HEK293 cells with plasmids expressing TMPRSS11A WT and human HAI-1 or HAI-2. In Western blotting of lysates from the transfected cells, we detected the ~ 37 -kDa TMPRSS11A band in cells co-expressing HAI-1 (Fig. 7, top panel). However, the level of the ~ 37 -kDa band was lower than that in control vector co-transfected cells. In cells co-expressing TMPRSS11A and HAI-2, the ~ 37 -kDa band was barely visible (Fig. 7, top panel). The ~ 28 -kDa TMPRSS11A band was not detected in cells co-expressing HAI-1 or HAI-2 (Fig. 7, top panel). These results indicate that HAI-2 is more potent than HAI-1 in inhibiting TMPRSS11A activity when co-expressed with TMPRSS11A in cells.

Discussion

TMPRSS11A is an airway epithelial TTSP implicated in SARS and MERS CoV infection (27, 28). For trypsin-like serine proteases, zymogen activation is essential for biological function (37). In this study, we examined the activation cleavage of human TMPRSS11A in HEK293 cells, esophageal cancer EC9706 cells, and lung epithelial 16HBE and A549 cells. Our results indicate that TMPRSS11A activation cleavage is mediated primarily by autocatalysis. This conclusion is supported by the findings that no activation cleavage was detected in catalytically inactive mutants R186A and S368A. In addition, TMPRSS11A WT, but not mutants R186A and S368A, cleaved the soluble TMPRSS11A mutant S368A, indicating that there were no other endogenous proteases capable of cleaving TMPRSS11A in the cells tested in our study. Moreover, our results show that TMPRSS11A activation cleavage occurs before the protease reaches the cell surface, as indicated by trypsin digestion, BFA, and monensin treatment, and intracellular cleavage of soluble TMPRSS11A. Together, our results reveal an intracellular autoactivation mechanism in converting one-chain TMPRSS11A zymogen into a two-chain enzyme.

Zymogen activation has been studied in TTSPs. To date, several distinct mechanisms have been identified. For example, hepsin and matriptase 2 (hepatic TTSPs) are autoactivated on the cell surface but not inside the cell (38–40). Corin (a cardiac TTSP) is activated in the extracellular space by proprotein convertase subtilisin/kexin-6 (6, 41). Enteropeptidase (an intestinal TTSP) is activated extracellularly and in a reciprocal manner in the presence of its substrate, trypsinogen (42). Similarly, epithelial matriptase activation is mediated by autocleavage, probably on the cell membrane (43), and by reciprocal activation with prostaticin, a glycosylphosphatidylinositol-anchored serine protease on the cell surface (44–46). More recently, activation cleavage of HAT and DESC1 (airway TTSPs) was observed in transfected cells (28); however, the responsible proteases (HAT and DESC1 versus unknown proteases) and the location of the cleavage (intracellular versus cell surface) are not defined. Together with our new findings of intracellular autoactivation cleavage in TMPRSS11A, these data show that molecular and cellular mechanisms in zymogen activation vary considerably among TTSPs.

TMPRSS11A was identified as a putative tumor suppressor in human esophageal cancers (32, 47). *TMPRSS11A* variants are linked to the risk of oral and esophageal squamous cell

TMPRSS11A zymogen activation

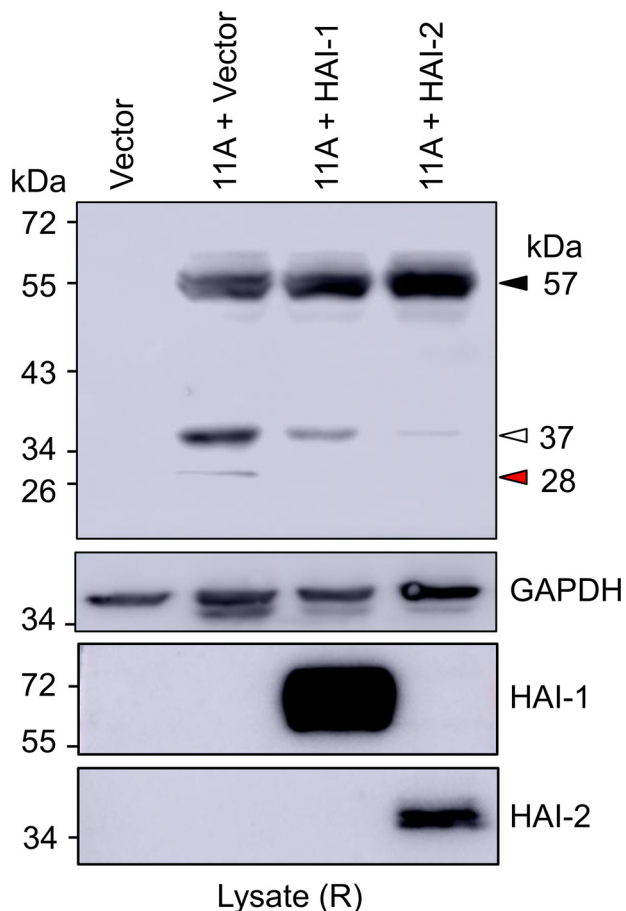


Figure 7. Effects of HAI-1 and HAI-2 expression on TMPRSS11A cleavage. HEK293 cells were transfected with a vector or plasmid expressing TMPRSS11A (11A) together with a vector or plasmids expressing human HAI-1 and HAI-2. TMPRSS11A fragments in cell lysates were analyzed by Western blotting under reducing (R) conditions with an anti-V5 antibody (top panel). GAPDH was used as a protein loading control (second panel). HAI-1 (third panel), and HAI-2 (bottom panel) protein expression in the transfected cells was verified in parallel Western blotting experiments using aliquots of the same lysate samples and an anti-FLAG antibody. Data are representative of at least three experiments.

carcinomas (31, 48, 49). To date, the physiological function of TMPRSS11A remains unclear. In mice, the *Tmprss11a* gene is co-localized with six other *Tmprss11* genes in a locus on chromosome 5E1 (50). Most of the *Tmprss11* genes are expressed in multiple epithelial tissues, including the trachea, esophagus, stomach, bladder, and skin (51, 52). *Tmprss11a*-deficient mice, however, did not exhibit noticeable defects in embryonic development and postnatal survival (51, 53). In humans, TMPRSS11A is expressed in the trachea (27, 28). In single-cell analysis, TMPRSS11A expression was detected in basal and secretory cells in human and mouse airway epithelia (30). In *Tmprss11a*-deficient mice, no apparent abnormalities were observed in trachea sections (51). These results indicate that TMPRSS11A is unnecessary for normal trachea structures but may have a regulatory function in the airway epithelium, which is yet identified.

Human airway epithelial proteases are important in CoV pathogenicity. By cleaving CoV S proteins between the S1/S2 and the S2' sites, the proteases enhance viral entry and cell-cell fusion in airway tissues (22, 54, 55). In purified protein-based

experiments, TMPRSS11A cleaved SARS-CoV S protein at both the S1/S2 and S2' sites (27). Similar TMPRSS11A-mediated cleavages of MERS-CoV S protein were observed in cell-based studies (28). In our study, we showed that TMPRSS11A cleaved the recombinant SARS-CoV-2 S protein extracellular fragment, producing an ~60-kDa band. A similar ~60-kDa band was also detected when sTMPRSS2 was used. Previously, the full-length SARS-CoV-2 S protein expressed in HEK293T cells was shown to be cleaved by furin at the S1/S2 site, generating an ~90-kDa band, consistent with the calculated molecular mass of a glycosylated S2 subunit (24). In that study, the S2' fragment with an expected molecular mass of 68 kDa (with glycosylation) was not detected. Together with previous reports (27, 28), the results from our study support a potential role of TMPRSS11A in CoV S protein cleavage. Additional studies will be important to verify the precise cleavage site in the SARS-CoV-2 S protein by TMPRSS11A. It is known that CoV S protein cleavage can occur at different locations in host cells: on the cell surface during virus entry, inside the cell during virus replication and S protein synthesis, and upon release from the cell (29, 54). In our study, we found activation-cleaved two-chain TMPRSS11A on the cell membrane and inside the cell. Further studies are required to determine whether and how TMPRSS11A enhances CoV infectivity in host cells.

Physiologically, protease activities are tightly regulated. In a previous study (28), TMPRSS11A-mediated cleavage of influenza A hemagglutinin was inhibited by a small molecule serine protease inhibitor, but not HAI-1, which inhibits several epithelial TTSPs (36). Moreover, co-expression of TMPRSS11A and HAI-1 in 293T cells reduced, but did not abolish, the cleavage of TMPRSS11A (28). Consistently, we found that HAI-1 was less effective than HAI-2 in blocking TMPRSS11A autoactivation cleavage when co-expressed in HEK293 cells. In single-cell analysis of the human airway epithelium, levels of *SPINT2* (encoding HAI-2) expression were ~2-fold higher than that of *SPINT1* (encoding HAI-1) (30). These results are consistent with our findings, indicating that HAI-2 is more important than HAI-1 in regulating TMPRSS11A activity in the respiratory track.

In summary, we examined the mechanism underlying TMPRSS11A zymogen activation cleavage. We show that TMPRSS11A activation cleavage is mediated primarily by autocatalysis that occurs before the protease reaches the cell surface. This intracellular autoactivation mechanism differs from the extracellular activation mechanism reported in other TTSPs. We also show that TMPRSS11A cleaved SARS-CoV-2 S protein in cell culture-derived medium. The results indicate that, in addition to TMPRSS2, other TTSPs in the respiratory system may also participate in SARS-CoV-2 infection. These findings should encourage more studies to understand the role of airway epithelial TTSPs in CoV infection.

Experimental procedures

Cell culture

HEK293 cells (ATCC, CRL-1573, authenticated by STR profiling) were cultured in Dulbecco's modified Eagle's medium (Corning, 10-0130CVRC) in the presence of 10% fetal

bovine serum (FBS) (Gibco, 16000-044). Human esophageal squamous cell carcinoma EC9706 cells were from Shanghai Fuxiang Biological Technology (Shanghai, China) and cultured in RPMI 1640 medium (Hyclone, sh30255) with 10% FBS. SV40-transfected human bronchial epithelial 16HBE cells and adenocarcinomic human alveolar basal epithelial A549 cells were from Ningbo Mingzhou Biological Technology (Ningbo, China; STR profiled) and cultured in minimum essential medium (Hyclone, SH300024) and RPMI 1640 medium, respectively, with 10% FBS. All cells were grown at 37°C with 5% CO₂.

Expression plasmids

Plasmids expressing human corin and hepsin were pcDNA 3.1/V5 (Thermo Fisher, K4800-01) based and encoded a C-terminal V5 tag, as described previously (40, 56). Full-length cDNAs encoding human TMPRSS11A and TMPRSS2 were amplified from myeloma (made in this study) and prostate (Clontech 636743) cDNA libraries, respectively, and inserted into the pcDNA 3.1/V5 plasmid to express TMPRSS11A and TMPRSS2. PCR-based site-directed mutagenesis (ClonExpress One Step Cloning kit) was carried out to make constructs expressing TMPRSS11A mutants R186A, R265A, and S368A. To express soluble forms of TMPRSS11A (sTMPRSS11A and sTMPRSS11A S368A), cDNA sequences encoding the extracellular regions of TMPRSS11A WT and the mutant S368A were amplified by PCR and inserted into pSecTag/FRT/V5 plasmid (Thermo Fisher, K6025-01) encoding an N-terminal Igκ signal peptide (35). Another pSecTag-based plasmid was made to express a soluble form of TMPRSS2 with the extracellular region (residues 106-492). All expressed TMPRSS11A proteins contained a C-terminal V5 tag. Human HAI-1 cDNA (106-1542 bp) and HAI-2 cDNA (84-759 bp) were amplified from a HEK293 cell-derived library and cloned into pcDNA 3.1 plasmid with an inserted 5' sequence encoding the CD33 signal peptide and a FLAG tag. A list of expression plasmids used in this study is included in Table S1.

Cell transfection

HEK293, EC9706, 16HBE, and A549 cells were cultured under the conditions described above. When the cells were at ~80% confluent, expression and control plasmids were transfected into the cells using PolyJet reagents (SigmaGen Laboratories, SL100688) at 37°C, based on the manufacturer's instructions. After 6 h of incubation, the cells were switched to fresh medium and incubated for 24-72 h before being used for further studies described below.

Flow cytometry

To verify cell surface expression of TMPRSS11A proteins, transfected HEK293 cells were detached from culture plates with 0.02% (w/v) EDTA without or with 0.25% (w/v) trypsin (Gibco, 25200). After being washed with serum-free medium, the cells were incubated with an anti-V5 antibody (Thermo Fisher, R96025, 1:1000) at 37°C for 1 h. After washing with PBS, an Alexa Fluor 488-labeled secondary antibody (Invitrogen, A21202, 1:500) was added to the cells and incubated at room temperature in the dark for 1 h. After washing, the cells

were analyzed with a flow cytometer (Gallios, Beckman). Pyridinium iodide (Sigma) was used for life gating. Data were analyzed with Kaluza software.

Immunostaining

HEK293 cells were cultured in 12-well-plates with glass coverslips (20 mm in diameter) and transfected with plasmids using PolyJet reagents at 37°C, as described above. After 6 h, the cells were switched to fresh medium. After 24 h, the cells were fixed with pre-cooled acetone (cell membrane permeabilized) or paraformaldehyde (4% v/v) (cell membrane not permeabilized) at room temperature for 5 min and incubated with 5% (w/v) BSA in PBS at 37°C for 1 h. After being washed with PBS, the cells were incubated with the anti-V5 antibody (described above) at 37°C for 1 h, followed by incubation with the Alexa Fluor 488-labeled secondary antibody (described above) at 37°C for 1 h. After washing, the coverslips were mounted with the 4',6-diamidino-2-phenylindole (DAPI) solution (Southern Biotech, 0100-20) and the cells were examined under a confocal microscope (Olympus, FV1000).

Western blotting

HEK293, EC9706, 16HBE, and A549 cells transfected with plasmids expressing TMPRSS11A proteins or a control vector were cultured, as described above. When the cell culture reached confluence, the conditioned medium was collected. TMPRSS11A proteins in the conditioned medium were immunoprecipitated using the anti-V5 antibody. The cells were lysed in a buffer containing 1% (v/v) Triton X-100, 50 mM Tris-HCl (pH 8.0), 150 mM NaCl, and a protease inhibitor mixture (1:100, Roche Applied Science, 04693116001). The proteins from the conditioned medium and cell lysates were mixed with a Laemmli sample buffer (Bio-Rad) with (reducing) or without (nonreducing) β-mercaptoethanol (2.5% v/v), and analyzed by SDS-PAGE and Western blotting using a horseradish peroxidase (HRP)-conjugated anti-V5 antibody (1:5000, Thermo Fisher, R96125). After incubation with a solution with an enhanced chemiluminescent substrate (NcmECL Ultra) (NCM Biotech, P10100), Western blots were exposed to a chemiluminescent imager (Amersham Biosciences Imager 600).

Biotin labeling of cell surface proteins

To label cell surface proteins, sulfo-NHS-biotin (0.25 mg/ml, Thermo Fisher) was added to cultured cells. After 4 min on ice, a glycine solution (100 mM) was added to stop the reaction. After 30 min, the cells were lysed, as described above. The biotin-labeled proteins were precipitated with NeutrAvidin beads (Thermo Fisher, 29201) at 4°C. After 16 h, proteins on the beads were eluted with the Laemmli buffer with or without β-mercaptoethanol (2.5%, v/v), and analyzed by SDS-PAGE and Western blotting, as described above.

PNGase F digestion

To examine N-linked glycans on TMPRSS11A, cell lysates or protein precipitates in a denaturing buffer (0.5% SDS and 40 mM DTT) were boiled for 10 min and treated with PNGase F

TMPRSS11A zymogen activation

(30 units, New England Biolabs, P0704), which removes *N*-linked oligosaccharides. After 3 h at 37 °C, the treated protein samples were analyzed by Western blotting using an anti-V5 antibody under reducing conditions, as described above.

Trypsin digestion of cell surface proteins

To examine proteins on HEK293 cell surface, transfected cells expressing TMPRSS11A and control cells expressing corin were treated with 0.25% (w/v) trypsin and 0.02% EDTA (w/v) (Gibco, 25200) at 37 °C for 30 s. Dulbecco's modified Eagle's medium with 10% FBS was added to neutralize trypsin activity. After washing with PBS, the cells were lysed in the lysis buffer as described above. Proteins were separated by SDS-PAGE under reducing conditions with 2.5% (v/v) β -mercaptoethanol in the Laemmli buffer. Western blotting was done using an HRP-conjugated anti-V5 antibody (1:5000, Thermo Fisher, R96125), as described above.

Brefeldin A and monensin treatment

To study the subcellular location of TMPRSS11A activation, HEK293 cells expressing TMPRSS11A and control cells expressing corin were treated with BFA (1 μ M) (Sigma, 203729-1MG) or monensin (0.3 μ M) (Sigma, 475897-100MG) to inhibit protein trafficking in the ER and the Golgi, respectively (34). After 20 h at 37 °C, the cells were washed and lysed. TMPRSS11A and corin proteins in the lysates were analyzed with Western blotting, as described above.

Cleavage of SARS-CoV-2 S protein extracellular fragment

To test the activity of TMPRSS11A forward SARS-CoV-2 S protein, sTMPRSS11A, sTMPRSS11A S368A (negative control), and sTMPRSS2 (positive control) were expressed in HEK293 cells. The conditioned media from the cells or vector-transfected control cells were collected and concentrated ~20-fold with a filter device. The concentrated media were incubated with a SARS-CoV-2 S protein extracellular domain (S-ECD) fragment (residues 16-1213) produced in insect cells and with a C-terminal FLAG tag (8 μ g/ml, Bioword Technology, NCP0030P). After 12 h at 37 °C, SARS-CoV-2 S-ECD and derived fragments were analyzed by Western blotting using an HRP-conjugated anti-FLAG antibody (Sigma, A8592, 1:10000).

Statistical analysis

Data were analyzed with Prism 6 software (Graphpad). Analysis of variance followed by Tukey's multiple comparison test was used to analyze data from three or more groups. *p* Values of <0.05 were considered to be statistically significant.

Data availability

All the data described in this study are contained within the article and accompanying [supporting information](#).

Author contributions—C. Z., N. D., and Q. W. conceptualization; C. Z. data curation; C. Z., N. D., and Q. W. formal analysis; C. Z. validation; C. Z., Y. Z., S. Z., Z. W., S. S., M. L., Y. C., and N. D. investigation; C. Z. and Q. W. visualization; C. Z., Y. Z., S. Z., Z. W.,

S. S., and Y. C. methodology; C. Z., N. D., and Q. W. writing-original draft; M. L. and N. D. supervision; M. L., N. D., and Q. W. project administration; N. D. resources; N. D. funding acquisition; N. D. and Q. W. writing-review and editing.

Funding and additional information—This work was supported in part by National Natural Science Foundation of China Grants 81873840 and 81873566 and the Priority Academic Program Development of Jiangsu Higher Education.

Conflict of interest—The authors declare that they have no conflicts of interest with the contents of this article.

Abbreviations—The abbreviations used are: TTSP, type II transmembrane serine protease; BFA, brefeldin A; CoV, coronavirus; DESC1, differentially expressed in squamous cell carcinoma 1; ECD, extracellular domain; ECRG1, esophageal cancer related gene 1; ER, endoplasmic reticulum; FBS, fetal bovine serum; HAI, hepatocyte growth factor activator inhibitor; HAT, human airway trypsin-like protease; HEK293, human embryonic kidney 293; MERS, Middle East respiratory syndrome; S, spike; SARS, severe acute respiratory syndrome; SEA, sea urchin sperm protein/enteropeptidase/agrin; TM, transmembrane; TMPRSS, transmembrane protease serine; GAPDH, glyceraldehyde-3-phosphate dehydrogenase; S-ECD, S protein extracellular domain fragment; HRP, horseradish peroxidase; TMPRSS2, transmembrane protease serine 2; PNGase F, peptide *N*-glycosidase F; DAPI, 4',6-diamidino-2-phenylindole.

References

1. Bugge, T. H., Antalis, T. M., and Wu, Q. (2009) Type II transmembrane serine proteases. *J. Biol. Chem.* **284**, 23177–23181 [CrossRef Medline](#)
2. Hooper, J. D., Clements, J. A., Quigley, J. P., and Antalis, T. M. (2001) Type II transmembrane serine proteases: insights into an emerging class of cell surface proteolytic enzymes. *J. Biol. Chem.* **276**, 857–860 [CrossRef Medline](#)
3. Heeney, M. M., and Finberg, K. E. (2014) Iron-refractory iron deficiency anemia (IRIDA). *Hematol. Oncol. Clin. North Am.* **28**, 637–652 [CrossRef Medline](#)
4. Stirnberg, M., and Gütschow, M. (2013) Matriptase-2, a regulatory protease of iron homeostasis: possible substrates, cleavage sites and inhibitors. *Curr. Pharm. Des.* **19**, 1052–1061 [CrossRef Medline](#)
5. Li, S., Peng, J., Wang, H., Zhang, W., Brown, J. M., Zhou, Y., and Wu, Q. (2020) Hepsin enhances liver metabolism and inhibits adipocyte browning in mice. *Proc. Natl. Acad. Sci. U.S.A.* **117**, 12359–12367 [CrossRef Medline](#)
6. Chen, S., Cao, P., Dong, N., Peng, J., Zhang, C., Wang, H., Zhou, T., Yang, J., Zhang, Y., Martelli, E. E., Naga Prasad, S. V., Miller, R. E., Malfait, A. M., Zhou, Y., and Wu, Q. (2015) PCSK6-mediated corin activation is essential for normal blood pressure. *Nat. Med.* **21**, 1048–1053 [CrossRef Medline](#)
7. Zhou, Y., and Wu, Q. (2014) Corin in natriuretic peptide processing and hypertension. *Curr. Hypertens. Rep.* **16**, 415 [CrossRef Medline](#)
8. Zheng, X. L., Kitamoto, Y., and Sadler, J. E. (2009) Enteropeptidase, a type II transmembrane serine protease. *Front. Biosci. (Elite Ed.)* **1**, 242–249 [Medline](#)
9. Guipponi, M., Antonarakis, S. E., and Scott, H. S. (2008) TMPRSS3, a type II transmembrane serine protease mutated in non-syndromic autosomal recessive deafness. *Front. Biosci.* **13**, 1557–1567 [CrossRef Medline](#)
10. Guipponi, M., Tan, J., Cannon, P. Z., Donley, L., Crewther, P., Clarke, M., Wu, Q., Shepherd, R. K., and Scott, H. S. (2007) Mice deficient for the type II transmembrane serine protease, TMPRSS1/hepsin, exhibit profound hearing loss. *Am. J. Pathol.* **171**, 608–616 [CrossRef Medline](#)
11. Cui, Y., Wang, W., Dong, N., Lou, J., Srinivasan, D. K., Cheng, W., Huang, X., Liu, M., Fang, C., Peng, J., Chen, S., Wu, S., Liu, Z., Dong, L., Zhou, Y.,

- et al.* (2012) Role of corin in trophoblast invasion and uterine spiral artery remodelling in pregnancy. *Nature* **484**, 246–250 [CrossRef Medline](#)
12. Miller, G. S., and List, K. (2013) The matriptase-prostasin proteolytic cascade in epithelial development and pathology. *Cell Tissue Res.* **351**, 245–253 [CrossRef Medline](#)
 13. Szabo, R., and Bugge, T. H. (2020) Membrane-anchored serine proteases as regulators of epithelial function. *Biochem. Soc. Trans.* **48**, 517–528 [CrossRef Medline](#)
 14. Buzza, M. S., Johnson, T. A., Conway, G. D., Martin, E. W., Mukhopadhyay, S., Shea-Donohue, T., and Antalis, T. M. (2017) Inflammatory cytokines down-regulate the barrier-protective prostasin-matriptase proteolytic cascade early in experimental colitis. *J. Biol. Chem.* **292**, 10801–10812 [CrossRef Medline](#)
 15. Lahey, K. A., Ronaghan, N. J., Shang, J., Dion, S. P., Désilets, A., Leduc, R., and MacNaughton, W. K. (2017) Signaling pathways induced by serine proteases to increase intestinal epithelial barrier function. *PLoS ONE* **12**, e0180259 [CrossRef Medline](#)
 16. Martin, C. E., and List, K. (2019) Cell surface-anchored serine proteases in cancer progression and metastasis. *Cancer Metastasis Rev.* **38**, 357–387 [CrossRef Medline](#)
 17. Tanabe, L. M., and List, K. (2017) The role of type II transmembrane serine protease-mediated signaling in cancer. *FEBS J.* **284**, 1421–1436 [CrossRef Medline](#)
 18. Bertram, S., Glowacka, I., Müller, M. A., Lavender, H., Gnirss, K., Nehlmeier, I., Niemeyer, D., He, Y., Simmons, G., Drosten, C., Soilleux, E. J., Jahn, O., Steffen, I., and Pöhlmann, S. (2011) Cleavage and activation of the severe acute respiratory syndrome coronavirus spike protein by human airway trypsin-like protease. *J. Virol.* **85**, 13363–13372 [CrossRef Medline](#)
 19. Zmora, P., Blazejewska, P., Moldenhauer, A. S., Welsch, K., Nehlmeier, I., Wu, Q., Schneider, H., Pöhlmann, S., and Bertram, S. (2014) DESC1 and MSPL activate influenza A viruses and emerging coronaviruses for host cell entry. *J. Virol.* **88**, 12087–12097 [CrossRef Medline](#)
 20. Gierer, S., Bertram, S., Kaup, F., Wrensch, F., Heurich, A., Krämer-Kühl, A., Welsch, K., Winkler, M., Meyer, B., Drosten, C., Dittmer, U., von Hahn, T., Simmons, G., Hofmann, H., and Pöhlmann, S. (2013) The spike protein of the emerging betacoronavirus EMC uses a novel coronavirus receptor for entry, can be activated by TMPRSS2, and is targeted by neutralizing antibodies. *J. Virol.* **87**, 5502–5511 [CrossRef Medline](#)
 21. Glowacka, I., Bertram, S., Müller, M. A., Allen, P., Soilleux, E., Pfefferle, S., Steffen, I., Tsegaye, T. S., He, Y., Gnirss, K., Niemeyer, D., Schneider, H., Drosten, C., and Pöhlmann, S. (2011) Evidence that TMPRSS2 activates the severe acute respiratory syndrome coronavirus spike protein for membrane fusion and reduces viral control by the humoral immune response. *J. Virol.* **85**, 4122–4134 [CrossRef Medline](#)
 22. Hoffmann, M., Kleine-Weber, H., Schroeder, S., Krüger, N., Herrler, T., Erichsen, S., Schiergens, T. S., Herrler, G., Wu, N. H., Nitsche, A., Müller, M. A., Drosten, C., and Pöhlmann, S. (2020) SARS-CoV-2 cell entry depends on ACE2 and TMPRSS2 and is blocked by a clinically proven protease inhibitor. *Cell* **181**, 271–280.e278 [CrossRef Medline](#)
 23. Matsuyama, S., Nao, N., Shirato, K., Kawase, M., Saito, S., Takayama, I., Nagata, N., Sekizuka, T., Katoh, H., Kato, F., Sakata, M., Tahara, M., Kutsuna, S., Ohmagari, N., Kuroda, M., *et al.* (2020) Enhanced isolation of SARS-CoV-2 by TMPRSS2-expressing cells. *Proc. Natl. Acad. Sci. U.S.A.* **117**, 7001–7003 [CrossRef Medline](#)
 24. Shang, J., Wan, Y., Luo, C., Ye, G., Geng, Q., Auerbach, A., and Li, F. (2020) Cell entry mechanisms of SARS-CoV-2. *Proc. Natl. Acad. Sci. U.S.A.* **117**, 11727–11734 [CrossRef Medline](#)
 25. Shirato, K., Kawase, M., and Matsuyama, S. (2013) Middle East respiratory syndrome coronavirus infection mediated by the transmembrane serine protease TMPRSS2. *J. Virol.* **87**, 12552–12561 [CrossRef Medline](#)
 26. Shulla, A., Heald-Sargent, T., Subramanya, G., Zhao, J., Perlman, S., and Gallagher, T. (2011) A transmembrane serine protease is linked to the severe acute respiratory syndrome coronavirus receptor and activates virus entry. *J. Virol.* **85**, 873–882 [CrossRef Medline](#)
 27. Kam, Y. W., Okumura, Y., Kido, H., Ng, L. F., Bruzzone, R., and Altmeyer, R. (2009) Cleavage of the SARS coronavirus spike glycoprotein by airway proteases enhances virus entry into human bronchial epithelial cells *in vitro*. *PLoS ONE* **4**, e7870 [CrossRef Medline](#)
 28. Zmora, P., Hoffmann, M., Kollmus, H., Moldenhauer, A. S., Danov, O., Braun, A., Winkler, M., Schughart, K., and Pöhlmann, S. (2018) TMPRSS11A activates the influenza A virus hemagglutinin and the MERS coronavirus spike protein and is insensitive against blockade by HAI-1. *J. Biol. Chem.* **293**, 13863–13873 [CrossRef Medline](#)
 29. Li, F. (2016) Structure, function, and evolution of coronavirus spike proteins. *Annu. Rev. Virol.* **3**, 237–261 [CrossRef Medline](#)
 30. Plasschaert, L. W., Žilionis, R., Choo-Wing, R., Savova, V., Knehr, J., Roma, G., Klein, A. M., and Jaffe, A. B. (2018) A single-cell atlas of the airway epithelium reveals the CFTR-rich pulmonary ionocyte. *Nature* **560**, 377–381 [CrossRef Medline](#)
 31. Li, Y., Zhang, X., Huang, G., Miao, X., Guo, L., Lin, D., and Lu, S. H. (2006) Identification of a novel polymorphism Arg290Gln of esophageal cancer related gene 1 (*ECRG1*) and its related risk to esophageal squamous cell carcinoma. *Carcinogenesis* **27**, 798–802 [CrossRef](#)
 32. Zhao, N., Huang, G., Guo, L., and Lu, S. H. (2006) *ECRG1*, a novel candidate of tumor suppressor gene in the esophageal carcinoma, triggers a senescence program in NIH3T3 cells. *Exp. Biol. Med. (Maywood)* **231**, 84–90 [CrossRef](#)
 33. Wang, H. T., Kong, J. P., Ding, F., Wang, X. Q., Wang, M. R., Liu, L. X., Wu, M., and Liu, Z. H. (2003) Analysis of gene expression profile induced by EMP-1 in esophageal cancer cells using cDNA microarray. *World J. Gastroenterol.* **9**, 392–398 [CrossRef Medline](#)
 34. Dinter, A., and Berger, E. G. (1998) Golgi-disturbing agents. *Histochem. Cell Biol.* **109**, 571–590 [CrossRef Medline](#)
 35. Knappe, S., Wu, F., Masikat, M. R., Morser, J., and Wu, Q. (2003) Functional analysis of the transmembrane domain and activation cleavage of human corin: design and characterization of a soluble corin. *J. Biol. Chem.* **278**, 52363–52370 [CrossRef Medline](#)
 36. Kataoka, H., Kawaguchi, M., Fukushima, T., and Shimomura, T. (2018) Hepatocyte growth factor activator inhibitors (HAI-1 and HAI-2): Emerging key players in epithelial integrity and cancer. *Pathol. Int.* **68**, 145–158 [CrossRef Medline](#)
 37. Huber, R., and Bode, W. (1978) Structural basis of the activation and action of trypsin. *Acc. Chem. Res.* **11**, 114–121 [CrossRef](#)
 38. Jiang, J., Yang, J., Feng, P., Zuo, B., Dong, N., Wu, Q., and He, Y. (2014) *N*-Glycosylation is required for matriptase-2 autoactivation and ectodomain shedding. *J. Biol. Chem.* **289**, 19500–19507 [CrossRef Medline](#)
 39. Stirnberg, M., Maurer, E., Horstmeyer, A., Kolp, S., Frank, S., Bald, T., Arenz, K., Janzer, A., Prager, K., Wunderlich, P., Walter, J., and Gütschow, M. (2010) Proteolytic processing of the serine protease matriptase-2: identification of the cleavage sites required for its autocatalytic release from the cell surface. *Biochem. J.* **430**, 87–95 [CrossRef Medline](#)
 40. Wang, L., Zhang, C., Sun, S., Chen, Y., Hu, Y., Wang, H., Liu, M., Dong, N., and Wu, Q. (2019) Autoactivation and calpain-1-mediated shedding of hepsin in human hepatoma cells. *Biochem. J.* **476**, 2355–2369 [CrossRef Medline](#)
 41. Chen, S., Wang, H., Li, H., Zhang, Y., and Wu, Q. (2018) Functional analysis of corin protein domains required for PCSK6-mediated activation. *Int. J. Biochem. Cell Biol.* **94**, 31–39 [CrossRef Medline](#)
 42. Lu, D., Yuan, X., Zheng, X., and Sadler, J. E. (1997) Bovine proenteropeptidase is activated by trypsin, and the specificity of enteropeptidase depends on the heavy chain. *J. Biol. Chem.* **272**, 31293–31300 [CrossRef Medline](#)
 43. Oberst, M. D., Williams, C. A., Dickson, R. B., Johnson, M. D., and Lin, C. Y. (2003) The activation of matriptase requires its noncatalytic domains, serine protease domain, and its cognate inhibitor. *J. Biol. Chem.* **278**, 26773–26779 [CrossRef Medline](#)
 44. Buzza, M. S., Martin, E. W., Driesbaugh, K. H., Desilets, A., Leduc, R., and Antalis, T. M. (2013) Prostasin is required for matriptase activation in intestinal epithelial cells to regulate closure of the paracellular pathway. *J. Biol. Chem.* **288**, 10328–10337 [CrossRef Medline](#)
 45. Friis, S., Uzzun Sales, K., Godiksen, S., Peters, D. E., Lin, C. Y., Vogel, L. K., and Bugge, T. H. (2013) A matriptase-prostasin reciprocal zymogen activation complex with unique features: prostasin as a non-enzymatic co-factor for matriptase activation. *J. Biol. Chem.* **288**, 19028–19039 [CrossRef Medline](#)

TMPRSS11A zymogen activation

46. Szabo, R., Lantsman, T., Peters, D. E., and Bugge, T. H. (2016) Delineation of proteolytic and non-proteolytic functions of the membrane-anchored serine protease prostaticin. *Development* **143**, 2818–2828 [CrossRef Medline](#)
47. Zhao, N., Wang, J., Cui, Y., Guo, L., and Lu, S. H. (2004) Induction of G1 cell cycle arrest and P15INK4b expression by ECRG1 through interaction with Miz-1. *J. Cell. Biochem.* **92**, 65–76 [CrossRef Medline](#)
48. Bachmann, K., Shahmiri, S., Kaifi, J., Schurr, P., Mann, O., Rawnaq, T., Block, S., Kalinin, V., Izbicki, J. R., and Strate, T. (2009) Polymorphism Arg290Arg in esophageal-cancer-related gene 1 (ECRG1) is a prognostic factor for survival in esophageal cancer. *J. Gastrointest. Surg.* **13**, 181–187 [CrossRef Medline](#)
49. Blessmann, M., Pohlenz, P., Atac, A., Kaifi, J. T., Eulenburg, C., Kalinin, V., Merkert, P., Smeets, R., Heiland, M., Blake, F., Schmelzle, R., and Izbicki, J. R. (2009) Single nucleotide polymorphism in esophageal cancer related gene 1: an analysis in resected oral squamous cell carcinoma patients. *Int. J. Oral Maxillofac. Surg.* **38**, 779–784 [CrossRef Medline](#)
50. Hobson, J. P., Netzel-Arnett, S., Szabo, R., Réhault, S. M., Church, F. C., Strickland, D. K., Lawrence, D. A., Antalis, T. M., and Bugge, T. H. (2004) Mouse DESC1 is located within a cluster of seven DESC1-like genes and encodes a type II transmembrane serine protease that forms serpin inhibitory complexes. *J. Biol. Chem.* **279**, 46981–46994 [CrossRef Medline](#)
51. Sales, K. U., Hobson, J. P., Wagenaar-Miller, R., Szabo, R., Rasmussen, A. L., Bey, A., Shah, M. F., Molinolo, A. A., and Bugge, T. H. (2011) Expression and genetic loss of function analysis of the HAT/DESC cluster proteases TMPRSS11A and HAT. *PLoS ONE* **6**, e23261 [CrossRef Medline](#)
52. Zhang, Z., Hu, Y., Yan, R., Dong, L., Jiang, Y., Zhou, Z., Liu, M., Zhou, T., Dong, N., and Wu, Q. (2017) The transmembrane serine protease HAT-like 4 is important for epidermal barrier function to prevent body fluid loss. *Sci. Rep.* **7**, 45262 [CrossRef Medline](#)
53. Callies, L. K., Tadeo, D., Simper, J., Bugge, T. H., and Szabo, R. (2019) Iterative, multiplexed CRISPR-mediated gene editing for functional analysis of complex protease gene clusters. *J. Biol. Chem.* **294**, 15987–15996 [CrossRef Medline](#)
54. Millet, J. K., and Whittaker, G. R. (2015) Host cell proteases: Critical determinants of coronavirus tropism and pathogenesis. *Virus Res.* **202**, 120–134 [CrossRef Medline](#)
55. Simmons, G., Zmora, P., Gierer, S., Heurich, A., and Pöhlmann, S. (2013) Proteolytic activation of the SARS-coronavirus spike protein: cutting enzymes at the cutting edge of antiviral research. *Antiviral Res.* **100**, 605–614 [CrossRef Medline](#)
56. Dong, N., Fang, C., Jiang, Y., Zhou, T., Liu, M., Zhou, J., Shen, J., Fukuda, K., Qin, J., and Wu, Q. (2013) Corin mutation R539C from hypertensive patients impairs zymogen activation and generates an inactive alternative ectodomain fragment. *J. Biol. Chem.* **288**, 7867–7874 [CrossRef Medline](#)